

# Universal Generalization Theory for Physical Intuitions from Small Artificial Neural Networks

Jingruo Peng<sup>1</sup>, Shuze Zhu<sup>\*1</sup>

<sup>1</sup>Center for X-Mechanics, Institute of Applied Mechanics, Zhejiang University, Hangzhou 310000, China

<sup>\*</sup>To whom correspondence should be addressed. E-mail: [shuzezhu@zju.edu.cn](mailto:shuzezhu@zju.edu.cn)

## Abstract

Physical intuitions are native functions from human brains, yet the understanding of how physical intuitions are formulated has remained elusive. In this Letter, we propose a mechanism that simulates how human brain can quickly develop intuitional understandings from limited observations. Conceiving a training algorithm adapted from the well-known variational principle in physics, small artificial neural networks can possess strong physical intuitions that master the problems of brachistochrone and quantum harmonic oscillators, by learning from a few highly similar samples. Our simulations suggest that the variational principle is the governing mechanism for artificial physical intuitions. A unified generalization theory is derived, which hinges upon a variational operation on the Euler-Lagrange equation. Our theory also rationalizes that there is a threshold of artificial neural network size below which satisfactory physical intuitions are not possible. Our work offers insights into how strong physical intuition can be formulated as humans or as artificial intelligences.

**Keywords:** Physics, machine learning, generalization, intuition learning

*Introduction* — Physical intuitions are essential part in our daily lives. For example, in ancient times, hunters threw a long stick with a spear at one end to kill animals. By a few trials, the physical intuitions come into play, so that a hunter would know how to adjust their throwing strategies towards a higher success rate. It is remarkable that our human brains can form intuitions based on only a few data points [1–3]. However, the mechanisms of how intuitions can be developed have remained elusive. Recently, artificial intelligence models (i.e., large language models, generative models) trained using large-scale data [4–17] has demonstrated performance comparable to or exceed human level, yet there is quite debate on whether these intricate models are truly as intelligent as humans [18,19]. In this Letter, we do not consider large-data models as we are interested in simulating the ability to learn quickly from limited observations [20,21]. In other words, can we utilize small artificial neural networks, trained from small data, to simulate and understand the formation process of strong physical intuitions?

Our understanding on the physical world is mainly based on the optimization of physical functionals, or equivalently, the variational principle. Evidence can be found not only in the classical physics but also in the quantum realm. It is thus reasonable to suspect that the variational principle is also the key for developing strong physical intuitions. To test this hypothesis, in this Letter, we conceive a variational learning method, adapted from the variational principle, to train small artificial neural networks (ANNs) to obtain intuitions over the basic problems of brachistochrone and quantum harmonic oscillators. The ANNs are first trained to learn a few observations, after which their parameters are frozen to make intuitive prediction on the previously unseen observations. The intuition performance is measured by the prediction accuracy over a wide range of previously unlearned samples. Such manner is majorly different from conventional physics-guided machine learning approaches [22–26]. Our results show that the variational-trained model’s intuition performance increases drastically with respect to the number of learned observations, in accordance with how humans develop intuitions just by learning a few cases. More importantly, only two highly similar observations are enough to boost a strong intuition, and there is a threshold size of ANN below which good intuition cannot be fostered. Our investigations propose a simple mechanism to explain how the biological neural network interprets the physical world.

*Logics of variational learning for intuitions* – Many laws of physics can be formulated as statements that some functional  $F[y]$  is optimized for certain  $y$ . If we consider perturbing  $y$  to some “nearby” function  $y(x) + \delta y(x)$ , and calculate the corresponding change in  $F$  as  $\delta F$  (to the first order of  $\delta y(x)$ ), then  $F$  is stationary at optimized state when  $\delta F = 0$  for all possible small variations  $\delta y$ . That is,

$$\lim_{\tau \rightarrow 0} \frac{1}{\tau} (F[y(x) + \tau \delta y(x)] - F[y(x)]) = 0 \quad (1)$$

Consider an artificial Agent equipped with an ANN labeled as  $y = NN(x, \zeta; W)$ . For a problem with observable physical feature  $\zeta$ , the Agent wants to learn the value of  $y$  at physical-domain coordinates denoted by  $x$ . The learning is accomplished by finding appropriate parameters  $W$ , so that  $y$  minimizes a physical functional  $F[y]$ . To learn a problem with a single observation feature  $\zeta_i$ , the Agent minimizes a loss function  $L = F[NN(x, \zeta_i; W_{i,t})]$  by updating  $W_{i,t}$  using back-propagation as the epoch  $t$  increases. After terminal epoch  $T$ , a stationary loss value can be obtained in-principle, where the corresponding  $y = NN(x, \zeta_i; W_{i,T})$  is the learnt result for observation  $\zeta_i$ .

However, in the context of intuition learning, we would like to train an Agent with  $y = NN(x, \zeta; W)$  that can produce reasonably accurate results for a wide set of  $\zeta_k$  given a single set of  $W$  that is learned from only a few observations. Mathematically, we would like to achieve the following

$$\sum_k \left| \lim_{\tau \rightarrow 0} \frac{1}{\tau} (F[NN(x, \zeta_k; W) + \tau \delta NN] - F[NN(x, \zeta_k; W)]) \right| = 0 \quad (2)$$

In ANN training, Eq. (2) can be implemented by correlating the perturbed functional with another observable physical feature  $\zeta_j$  as in Eq. (3), where  $\tau_{k,j}$  represents the closeness between observations

$$\sum_{k,j} \left| \lim_{\tau_{k,j} \rightarrow 0} \frac{1}{\tau_{k,j}} (F[NN(x, \zeta_j; W)] - F[NN(x, \zeta_k; W)]) \right| \cong 0 \quad (3)$$

Then, we introduce our variational learning approach. In practice, if the Agent is allowed to learn from two observations  $\zeta_k$  and  $\zeta_j$ , Eq. (3) can be implemented by letting the Agent minimize  $L_{k,t} = F[NN(x, \zeta_k; W_t)]$  at odd epoch  $t$  and minimize  $L_{j,t} = F[NN(x, \zeta_j; W_t)]$  at even epoch  $t$ . Note that each neighboring epoch deals with a different loss function with shared learnable parameter set  $W_t$ , which is updated only once at a single epoch  $t$ . After terminal epoch  $T$ , two stationary Loss values can be obtained in-principle, where the corresponding  $y =$

$NN(x, \zeta_k; W_T)$  and  $y = NN(x, \zeta_j; W_T)$  are the learnt result for observation  $\zeta_k$  and  $\zeta_j$ . These stationary loss values guarantee that the absolute differences among Loss values are minimized, which is a necessary condition for Eq. (3). If more observations are used for training, then at each epoch, the Agent can choose a Loss functional of random sequence of observations to minimize.

To test intuition for previously unlearned observation  $\zeta_p$ , the result predicted by the Agent  $y = NN(x, \zeta_p; W_T)$ , where the  $W_T$  is trained using previously learned observations, is compared with the ground truth solution. The tested intuition is defined to be good if the correlation coefficient  $R^2$  between the guessed result and the ground-truth solution exceeds a threshold value. In the Letter, the threshold value for good-intuition is 90%.

*Brachistochrone* — The objective is to find the fastest trajectory of a particle to travel from  $(0, 0)$  to  $(X^*, H^*)$  only by the effect of gravity (along positive  $Y$  direction), represented by an ANN  $y = NN(x, X^*, H^*; W)$  for every  $X$ -coordinate  $x$ . Figure 1(a) shows the discretized ground-truth trajectories for three highly similar observations  $(X^*, H^*)$ . The underlying physics of each observation is embedded in the loss function  $L(X^*, H^*; W)$ , which describes the total travel time passing each segment plus the boundary penalty. To learn from the single observation of fixed  $(X^*, H^*)$  the Agent minimizes  $L(X^*, H^*; W_t)$  by updating  $W_t$  using back-propagation as the epoch  $t$  increases. To learn from multiple observations of varying  $(X^*, H^*)$ , the Agent invokes the variational learning approach (as described in previous section) by updating the shared  $W_t$  as the input feature  $(X^*, H^*)$  changes every single epoch. Figures 1(b-d) exhibits the map of good intuition (see definition in previous section) in the space spanned by  $X^*$  and  $H^*$  after the Agent learns different sets of  $W_T$  from single, double, and triple observations. The map is obtained by comparing  $y = NN(x, X^*, H^*; W_T)$  with ground-truth trajectory for a particular  $(X^*, H^*)$ . For all  $W_T$  trained from single observation, its good-intuition region has a slender shape. However, the good-intuition regions trained from double observations (e.g., Figures 1(b-c)) enlarge drastically when compared with those from corresponding single observation, and the good-intuition region (Figure 1(d)) trained from triple observations is the largest.

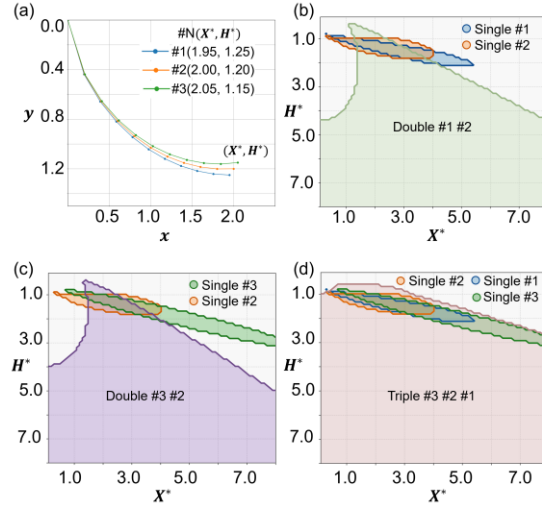


Figure 1. (a) Discretized ground truth brachistochrone trajectories for three highly similar observations labeled by the ending point coordinates  $(X^*, H^*)$ . Here the  $y$ -axis point downwards along the gravity direction. (b) Comparisons of good-intuition regions learnt from single observation #1, single observation #2, and variational double observations #1 #2. (c) Comparisons of good-intuition regions learnt from single observation #2, single observation #3, and variational double observations #2 #3. (d) Comparisons of good-intuition regions learnt from single observation #1, single observation #2, observation #3, and variational triple observations #1 #2 #3. Note that in (b-d) the parametric space is spanned by  $X^*$  and  $H^*$ .

*Quantum harmonic oscillators* – Consider the one-dimensional harmonic oscillator in quantum mechanics, whose potential energy function is  $V(x) = \frac{1}{2}m^*\omega^*x^2$ . The Agent wants to learn the ground state coupled to the observation  $(m^*, \omega^*)$ . The wavefunction to be learned is represented by an ANN  $\psi = NN(x, m^*, \omega^*; W)$  for every  $X$ -coordinate  $x$ . Figure 2(a) shows the discretized ground-truth trajectories for three highly similar observations  $(m^*, \omega^*)$ . The loss function  $L(m^*, \omega^*; W)$  associated with each observation is the Hamiltonian expectation  $\langle \psi | H | \psi \rangle / \langle \psi | \psi \rangle$ . Again, the Agent learns from single observation, or from multiple observations using the variational learning method. Figures 2(b-d) exhibits the map of good intuition in the space spanned by  $m^*$  and  $\omega^*$  after the Agent learns different sets of  $W_T$  from single, double, and triple observations. For all  $W_T$  trained from single observation, its good-intuition region is highly localized. In contrast, the good-intuition regions trained from double observations (e.g., Figures 2(b-c)) enlarge drastically, and the good-intuition region (Figure 2(d)) trained from triple observations is the largest.

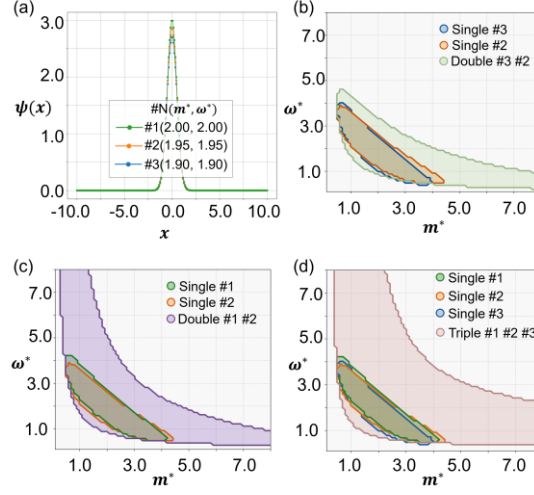


Figure 2. (a) Discretized ground-state wavefunctions of quantum harmonic oscillators for three highly similar observations labeled by system parameters  $(m^*, \omega^*)$ . (b) Comparisons of good-intuition regions learnt from single observation #2, single observation #3, and variational double observations #2 #3. (c) Comparisons of good-intuition regions learnt from single observation #1, single observation #2, and variational double observations #1 #2. (d) Comparisons of good-intuition regions learnt from single observation #1, single observation #2, observation #3, and variational triple observations #1 #2 #3. Note that in (b-d) the parametric space is spanned by  $m^*$  and  $\omega^*$ .

*Unified generalization theory* – The above universal performance of developing physical intuitions from classic and quantum physics regimes suggests the existence of a unified generalization theory. We first show that these optimization problems share the stationary conditions of similar mathematical structure. For Brachistochrone, it is standard knowledge that the Euler-Lagrange equations govern the problem of brachistochrone. That is, the stationary condition is  $\frac{\partial F}{\partial y} - \frac{d}{dx} \frac{\partial F}{\partial y'} = 0$  when the functional  $\int F(x, y, y') dx$  is optimized. For the quantum harmonic oscillator, the functional to be optimized is  $\int \psi^* H \psi dx$  with the constraint  $\int \psi^* \psi dx = 1$  where the Hamiltonian operator is  $H = -\frac{\hbar^2}{2m} \frac{\partial^2}{\partial x^2} + V$ . Note that  $\int \psi^* \frac{\partial^2}{\partial x^2} \psi dx = -\int \frac{\partial}{\partial x} \psi^* \cdot \frac{\partial}{\partial x} \psi dx = -\int \psi^{*'} \cdot \psi' dx$  because  $\psi$  vanishes when  $x \rightarrow \pm\infty$ . Introducing Lagrange multiplier  $\lambda$ , we then find the extremum of the functional  $\int S(x, \psi, \psi') dx = \int \left[ \frac{\hbar^2}{2m} \psi^{*'} \cdot \psi' + \psi^* V \psi - \lambda \psi^* \psi \right] dx$  according to the Euler-Lagrange equation  $\frac{\partial S}{\partial \psi} - \frac{d}{dx} \frac{\partial S}{\partial \psi'} = 0$  and  $\frac{\partial S}{\partial \psi^*} - \frac{d}{dx} \frac{\partial S}{\partial \psi^{*'}} = 0$ , which reduce to Schrödinger's equation  $H\psi = \lambda\psi$ .

Then, we reveal the underlying governing physics of generalization due to variational principle. The similar mathematical structure of the stationary conditions (i.e., the Euler-Lagrange equations) can be generically described as

$$\frac{\partial F(x, y(x, \zeta), y'(x, \zeta))}{\partial y} - \frac{d}{dx} \frac{\partial F(x, y(x, \zeta), y'(x, \zeta))}{\partial y'} = 0 \quad (4)$$

with encoded observation feature  $\zeta$ . If the observation feature  $\zeta = \zeta_0$  is perturbed by  $\delta\zeta$ , we then derive the condition

for the following Eq. (5) to hold.

$$\frac{\partial F(x, y(x, \zeta_0 + \delta\zeta), y'(x, \zeta_0 + \delta\zeta))}{\partial y} - \frac{d}{dx} \frac{\partial F(x, y(x, \zeta_0 + \delta\zeta), y'(x, \zeta_0 + \delta\zeta))}{\partial y'} = 0 \quad (5)$$

To the first order approximation, from  $y(x, \zeta_0 + \delta\zeta) = y(x, \zeta_0) + \frac{\partial y}{\partial \zeta} \delta\zeta$ ,  $y'(x, \zeta_0 + \delta\zeta) = y'(x, \zeta_0) + \frac{\partial y'}{\partial \zeta} \delta\zeta$ , we have

$$F(x, y(x, \zeta_0 + \delta\zeta), y'(x, \zeta_0 + \delta\zeta)) = F(x, y(x, \zeta_0), y'(x, \zeta_0)) + \frac{\partial F}{\partial y} \frac{\partial y}{\partial \zeta} \delta\zeta + \frac{\partial F}{\partial y'} \frac{\partial y'}{\partial \zeta} \delta\zeta \quad (6)$$

Utilizing the condition that Eq. (4) holds at  $\zeta = \zeta_0$ , then Eq. (5) transforms to

$$\frac{\partial \left( \frac{\partial F}{\partial y} \frac{\partial y}{\partial \zeta} \delta\zeta + \frac{\partial F}{\partial y'} \frac{\partial y'}{\partial \zeta} \delta\zeta \right)}{\partial y} - \frac{d}{dx} \frac{\partial \left( \frac{\partial F}{\partial y} \frac{\partial y}{\partial \zeta} \delta\zeta + \frac{\partial F}{\partial y'} \frac{\partial y'}{\partial \zeta} \delta\zeta \right)}{\partial y'} = 0 \quad (7)$$

Note that the finite perturbation  $\delta\zeta$  can be eliminated from the equation. Exchanging the orders of partial derivatives, Eq. (7) can be further simplified to

$$\frac{\partial}{\partial \zeta} \left( \frac{\partial F}{\partial y} - \frac{d}{dx} \frac{\partial F}{\partial y'} \right) = 0 \quad (8)$$

Eq. (8) encodes the core of our proposed generalization theory. It requires vanishing the derivative of the Euler-Lagrange equation with respect to the observation feature. Apparently, the above reasoning can be extended to generalized Euler-Lagrange equation, when treating multiple variables or systems of equations.

In practical implementation of the variational learning (i.e., Eq. (3)), the consequence of training a single ANN to achieve joint stationary conditions is equivalent to letting the ANN learn to satisfy not only  $\left| \frac{\partial}{\partial \zeta} \left( \frac{\partial F}{\partial y} - \frac{d}{dx} \frac{\partial F}{\partial y'} \right) \right| < \varepsilon$  when switching among observations but also  $\left| \frac{\partial F}{\partial y} - \frac{d}{dx} \frac{\partial F}{\partial y'} \right| < \varepsilon$  when focusing on a single observation, where  $\varepsilon$  is a small number. The quality of intuition generalization for previously unlearned observation can be assessed using a slightly enlarged  $\varepsilon$ . Therefore, our conceived variational learning method has a strong theoretical basis.

*Threshold for generalization* – The above generalization theory implies that the number of parameters in the ANN must exceed a threshold value in order to obtain satisfactory generalization for physical intuition. We define the generalization metric as the area of good-intuition regions within the tested observation feature range (i.e., those shaded area in Figure 1(b-d)). Figure 3 shows that for all the previously discussed problems, the critical number of parameters that obviously increases the generalization metric when learning from triple observations is around 100 to 150. In fact, such an order of magnitude of critical number of parameters can be rationalized using our generalization theory. For the brachistochrone (Figure 1(a)), the trajectory is described by 11 allocation points (including boundary points). During

triple-observation variational learning, at each allocation point, not only  $\left| \frac{\partial F}{\partial y} - \frac{d}{dx} \frac{\partial F}{\partial y'} \right| < \varepsilon$  but also  $\left| \frac{\partial}{\partial \zeta} \left( \frac{\partial F}{\partial y} - \frac{d}{dx} \frac{\partial F}{\partial y'} \right) \right| < \varepsilon$  would be satisfied. As a result, the former condition renders  $11 \times 3$  constraints, while the latter condition renders  $11 \times 6$  constraints (note that there are 6 ways of selecting ordered pair out of three observations). Since each observation has 2 boundary constraints, there are additional  $2 \times 3$  constraints. In total, there are 102 constraints to be satisfied by the ANN during triple-observation variational learning. Therefore, the above estimation can already rationalize the critical number of parameters to be on the order of 100. Particular attention should be paid to the analysis on the quantum harmonic oscillator problem (Figure 2(a)), as the flat (vanishing) portions of the wave function are sample-independent. Therefore, about 12 allocation points on the symmetric half of the non-vanishing portions are physically important to distinguish among observations, which would render about 118 constraints to be satisfied by the ANN during triple-observation variational learning, so that again the critical number of parameters is rationalized to be on the order of 100.

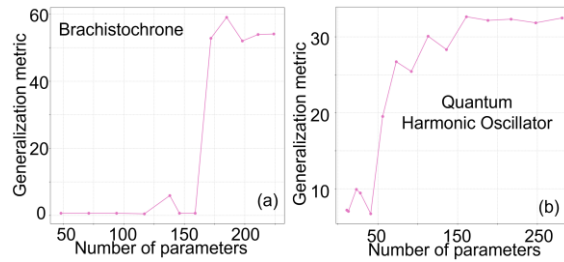


Figure 3. The evolution of generalization metric as a function of number of parameters in artificial neural networks. (a) Brachistochrone. (b) Quantum harmonic oscillator.

*Conclusions* – Inspired by the variational principle in physics, we conceive a machine learning algorithm of variational learning for physical intuitions, with successful demonstrations in problems of brachistochrone and quantum harmonic oscillators. Utilizing small artificial neural networks with the number of parameters on the order of 100, strong generalization performance for accurate physical intuitions is possible. A universal generalization theory is thus proposed, emphasizing on vanishing the derivative of the Euler-Lagrange equation with respect to observation feature. Our theory further establishes that there exists a threshold value of the size of the artificial neural network below which satisfactory intuition generalization cannot be achieved. Our work not only contributes to the understanding of the generalization ability from artificial intelligence, but also offers potential insights into how humans perceive the physical world that are governed by the optimization of physical functionals.



## Reference

- [1] B. M. Lake, T. D. Ullman, J. B. Tenenbaum, and S. J. Gershman, Building machines that learn and think like people, *Behav. Brain Sci.* **40**, e253 (2017).
- [2] Y. Wang, Q. Yao, J. T. Kwok, and L. M. Ni, Generalizing from a Few Examples: A Survey on Few-shot Learning, *ACM Comput. Surv.* **53**, 1 (2021).
- [3] L. He, Y. Xu, W. He, Y. Lin, Y. Tian, Y. Wu, W. Wang, Z. Zhang, J. Han, Y. Tian, B. Xu, and G. Li, Network model with internal complexity bridges artificial intelligence and neuroscience, *Nat. Comput. Sci.* **4**, 584 (2024).
- [4] P. Ma, S. Petridis, and M. Pantic, Visual speech recognition for multiple languages in the wild, *Nat. Mach. Intell.* **4**, 930 (2022).
- [5] W. X. Zhao, K. Zhou, J. Li, T. Tang, X. Wang, Y. Hou, Y. Min, B. Zhang, J. Zhang, Z. Dong, Y. Du, C. Yang, Y. Chen, Z. Chen, J. Jiang, R. Ren, Y. Li, X. Tang, Z. Liu, P. Liu, J.-Y. Nie, and J.-R. Wen, *A Survey of Large Language Models*.
- [6] A. M. Rahmani, E. Azhir, S. Ali, M. Mohammadi, O. H. Ahmed, M. Yassin Ghafour, S. Hasan Ahmed, and M. Hosseinzadeh, Artificial intelligence approaches and mechanisms for big data analytics: a systematic study, *PeerJ Comput. Sci.* **7**, e488 (2021).
- [7] J. S.-I. Kwon, Adding big data into the equation, *Nat. Chem. Eng.* **1**, 724 (2024).
- [8] A. M. Schweidtmann, E. Esche, A. Fischer, M. Kloft, J. Repke, S. Sager, and A. Mitsos, Machine Learning in Chemical Engineering: A Perspective, *Chem. Ing. Tech.* **93**, 2029 (2021).
- [9] K. Swanson, G. Liu, D. B. Catacutan, A. Arnold, J. Zou, and J. M. Stokes, Generative AI for designing and validating easily synthesizable and structurally novel antibiotics, *Nat. Mach. Intell.* **6**, 338 (2024).
- [10] H. Wang, T. Fu, Y. Du, W. Gao, K. Huang, Z. Liu, P. Chandak, S. Liu, P. Van Katwyk, A. Deac, A. Anandkumar, K. Bergen, C. P. Gomes, S. Ho, P. Kohli, J. Lasenby, J. Leskovec, T.-Y. Liu, A. Manrai, D. Marks, B. Ramsundar, L. Song, J. Sun, J. Tang, P. Veličković, M. Welling, L. Zhang, C. W. Coley, Y. Bengio, and M. Zitnik, Scientific discovery in the age of artificial intelligence, *Nature* **620**, 47 (2023).
- [11] M. Reichstein, G. Camps-Valls, B. Stevens, M. Jung, J. Denzler, N. Carvalhais, and Prabhat, Deep learning and process understanding for data-driven Earth system science, *Nature* **566**, 195 (2019).
- [12] Y. LeCun, Y. Bengio, and G. Hinton, Deep learning, *Nature* **521**, 436 (2015).
- [13] D. Silver, A. Huang, C. J. Maddison, A. Guez, L. Sifre, G. Van Den Driessche, J. Schrittwieser, I. Antonoglou, V. Panneershelvam, M. Lanctot, S. Dieleman, D. Grewe, J. Nham, N. Kalchbrenner, I. Sutskever, T. Lillicrap, M. Leach, K. Kavukcuoglu, T. Graepel, and D. Hassabis, Mastering the game of Go with deep neural networks and tree search, *Nature* **529**, 484 (2016).
- [14] L. Xiao, F. Zhang, and F. Zhao, Large-scale microbiome data integration enables robust biomarker identification, *Nat. Comput. Sci.* **2**, 307 (2022).
- [15] W. Liang, G. A. Tadesse, D. Ho, L. Fei-Fei, M. Zaharia, C. Zhang, and J. Zou, Advances, challenges and opportunities in creating data for trustworthy AI, *Nat. Mach. Intell.* **4**, 669 (2022).
- [16] J. Dauparas, I. Anishchenko, N. Bennett, H. Bai, R. J. Ragotte, L. F. Milles, B. I. M. Wicky, A. Courbet, R. J. De Haas, N. Bethel, P. J. Y. Leung, T. F. Huddy, S. Pellock, D. Tischer, F. Chan, B. Koepnick, H. Nguyen, A. Kang, B. Sankaran, A. K. Bera, N. P. King, and D. Baker, Robust deep learning-based protein sequence design using ProteinMPNN, *Science* **378**, 49 (2022).
- [17] B. Peters and N. Kriegeskorte, Capturing the objects of vision with neural networks, *Nat. Hum. Behav.* **5**, 1127 (2021).
- [18] M. Steyvers, H. Tejeda, A. Kumar, C. Belem, S. Karny, X. Hu, L. W. Mayer, and P. Smyth, What large language models know and what people think they know, *Nat. Mach. Intell.* **7**, 221 (2025).
- [19] A. Chemero, LLMs differ from human cognition because they are not embodied, *Nat. Hum. Behav.* **7**, 1828 (2023).
- [20] C. Zhang, B. Jia, Y. Zhu, and S.-C. Zhu, Human-level few-shot concept induction through minimax entropy learning, *Sci. Adv.* **10**, eadg2488 (2024).
- [21] B. M. Lake and M. Baroni, Human-like systematic generalization through a meta-learning neural network, *Nature* **623**, 115 (2023).
- [22] S. Cai, Z. Mao, Z. Wang, M. Yin, and G. E. Karniadakis, Physics-informed neural networks (PINNs) for fluid mechanics: a review, *Acta Mech. Sin.* **37**, 1727 (2021).

- [23] M. Raissi, P. Perdikaris, and G. E. Karniadakis, Physics-informed neural networks: A deep learning framework for solving forward and inverse problems involving nonlinear partial differential equations, *J. Comput. Phys.* **378**, 686 (2019).
- [24] W. E and B. Yu, The Deep Ritz Method: A Deep Learning-Based Numerical Algorithm for Solving Variational Problems, *Commun. Math. Stat.* **6**, 1 (2018).
- [25] E. Samaniego, C. Anitescu, S. Goswami, V. M. Nguyen-Thanh, H. Guo, K. Hamdia, X. Zhuang, and T. Rabczuk, An energy approach to the solution of partial differential equations in computational mechanics via machine learning: Concepts, implementation and applications, *Comput. Methods Appl. Mech. Eng.* **362**, 112790 (2020).
- [26] D. W. Abueidda, Q. Lu, and S. Koric, Meshless physics-informed deep learning method for three-dimensional solid mechanics, *Int. J. Numer. Methods Eng.* **122**, 7182 (2021).